Adv. Geosci., 40, 11–17, 2014
www.adv-geosci.net/40/11/2014/
doi:10.5194/adgeo-40-11-2014

Advances in Geosciences
Open Access

Retrieval of Ocean Bottom and Downhole Seismic sensors orientation using integrated MEMS gyroscope and direct rotation measurements

A. D'Alessandro and G. D'Anna

Istituto Nazionale di Geofisica e Vulcanologia, Centro Nazionale Terremoti, Italy

Correspondence to: A. D'Alessandro (antonino.dalessandro@ingv.it)

Received: 30 June 2014 – Revised: 30 October 2014 – Accepted: 6 November 2014 – Published: 15 December 2014

Abstract. The absolute orientation of the horizontal components of ocean bottom or downhole seismic sensors are generally unknown. Almost all the methods proposed to overcome this issue are based on the post-processing of the acquired signals and so the results are strongly dependent on the nature, quantity and quality of the acquired data. We have carried out several test to evaluate the ability of retrieve sensor orientation using integrated low cost MEMS gyroscope. Our tests have shown that the tested MEMS gyroscope (the model 1044_0–3/3/3 Phidget Spatial Precision High Resolution) can be used to measure angular displacement and therefore to retrieve the absolute orientation of the horizontal components of a sensor that has been subjected to rotation in the horizontal plane. A correct processing of the acquired signals permit to retrieve, for rotation at angular rate between 0 and 180° s^{-1}, angular displacement with error less 2°.

1 Introduction

Ocean Bottom Seismometers (OBS) are fundamental tools for the monitoring and study of seismogenetic offshore areas (D'Alessandro et al., 2009, 2012a, 2013a, 2014a; D'Alessandro, 2014a). An OBS is a stand-alone seismic station that can be deployed in open sea until a depth of several kilometres (Mangano et al., 2011). During the OBS descent phase along the seawater column, the seismic sensor can be undergo to random rotations on the horizontal plane. How and how much the sensor has rotated before reaching the ocean bottom is unknown and so it is not possible to retrieve the correct orientation of the its horizontal components. Similar problem can occur in the installation of seismic sensor in deep borehole. Indeed, to reduce the background noise level, seismic sensors are often installed on downhole, at depths of several tens of meters. The orientation of the sensor is usually determined with a gyroscopic tool that is lowered into the hole and into the keyed hole-lock (Holcomb, 2002). However, the gyro tools are relatively fragile and very expensive (Holcomb, 2002). For these reasons, several authors have proposed alternative cheaper methods for orienting borehole sensors.

Almost all the methods proposed to retrieve the correct horizontal components orientation, are based on the post-processing of the acquired signals (Anderson et al., 1987; Duennebier et al., 1987; Nakamura et al., 1987; Chiu et al., 1994; Michaels, 2001; Baker and Stevens, 2004; Oye and Ellsworth, 2005; Zheng and McMechan, 2006; Ekström and Busby, 2008; D'Alessandro et al., 2009, 2013a; Grigoli et al., 2012; Stachnik et al., 2012; Ringler et al., 2012, 2013; Zha et al., 2013). These techniques employ different approaches (polarization analysis, cross-correlation measurements, synthetic seismograms fitting), different datasets (shots, earthquakes, seismic noise) using different part of the seismic wave-field (P or S wave arrival times, Rayleigh waves, full waveforms), but are all based on the post-processing of the acquired data. Anderson et al. (1987), Duennebier et al. (1987) and Nakamura et al. (1987) used the amplitude ratio of water waves and first arrivals generated by air gun shots from known locations to orientate OBS. Chiu et al. (1994) used the late arrivals times (mainly S wave) to orientate strong motion sensors installed on borehole. Michaels (2001) proposed a method based on principal component analysis to determine the sensors orientation, relative to source polarization direction using SH wave. Holcomb (2002) test several techniques

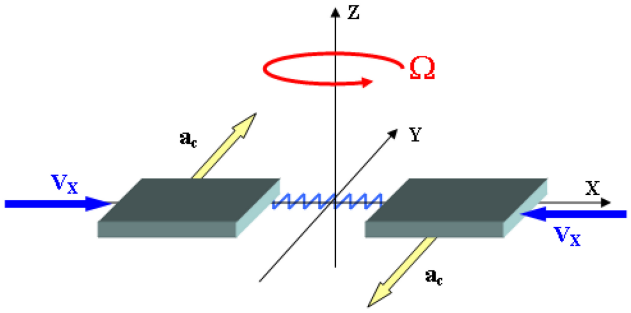

Figure 1. Sketch of the principle of operation of a MEMS gyroscope.

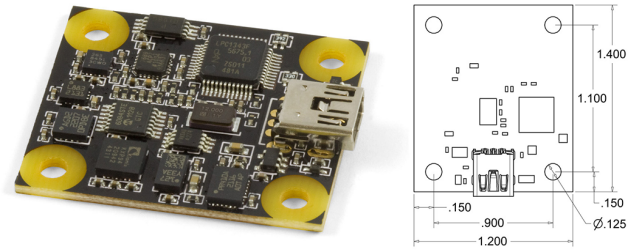

Figure 2. MEMS model 1044_0 (3/3/3 PhidgetSpatial Precision High Resolution) produced by the Canadian company Phidget Inc.; the reported measures are in inches.

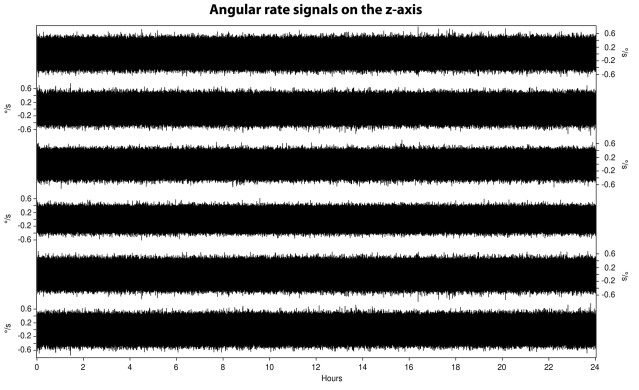

Figure 3. 24 h angular rate signals (z axis) recorded by the six MEMS gyroscope here tested.

based on the comparison of the sensor signal outputs with that of a reference-oriented sensor. The methods proposed by Baker and Stevens (2004) and also adopted by Stachnik et al. (2012), is based on the polarization of observed Rayleigh-waves. Oye and Ellsworth (2005) determined sensors absolute orientations comparing azimuths obtained from P wave polarization analysis and theoretical azimuths estimated from ray-tracing. Zheng and McMechan (2006) used traces cross-correlation to infer relative angles between adjacent geophone pairs in borehole arrays. Ekström and Busby (2008) determine sensor orientation by examining correlations between observed and synthetic surface-wave over a range of orientations. D'Alessandro et al. (2009, 2013a) employed a method based on noise unbiased polarization analysis of the first P-wave arrival time of well-located events. Grigoli et al. (2012) proposed a complex linear least-squares method applicable on full waveform records. Ringler et al. (2012, 2013) developed a technique for estimating relative sensor azimuths by inverting for the orientation with the maximum correlation to a reference instrument, using a non-linear parameter estimation routine. Zha et al. (2013) proposed a method based on polarization analysis of Rayleigh waves retrieved from ambient noise cross-correlation.

However, all these methods are not error-free and not always applicable: methods based on active sources are not applicable in seismic passive monitoring campaigns; methods based on synthetic waveforms are strong dependent on accuracy of the source parameters estimations and are generally computationally intensive; methods based on polarization analysis are clearly strong dependent on the quality of the data in term of number of seismic events recorded, azimuthal coverage and signal to noise ratio; methods base on events or noise cross-correlation can be applicable only if an array of sensor is deployed, but are not applicable to individual sensors or sensor-very far from each other.

For all the above reasons it would be desirable a not expensive direct method for the determination of the absolute orientation of the sensor horizontal components, not dependent on the nature, quantity and quality of the data acquired. The simplest solution to this problem would be the installation, together with the sensors, of an electronic compass able to measure the real horizontal component orientation respect to the magnetic North. However, as well known, all the seismic sensors currently used in earthquakes monitoring produces moderate to strong electromagnetic fields, which make the data recorded by an electronic compass, placed in their proximity, unusable for the described purpose.

For this reason, in this work we propose an alternative method for the estimation of the absolute orientation of horizontal components of a sensor, based on the use of MEMS (Micro Electro-Mechanical Systems) gyroscope.

In the following sections, after describing in detail the technical characteristics of the MEMS gyroscope, we will describe the tests carried out to verify the suitability of this device in determining the actual orientation of the horizontal components of a seismic sensor placed on downhole or on ocean bottom.

2 MEMS gyroscopes

MEMS devices have been recognized as one of the most promising technologies of the XXI century, able to revolutionize both the industrial world and that of the consumer products. In the 90s, MEMS sensors revolutionized the automotive airbag system and are today widely used in lap-

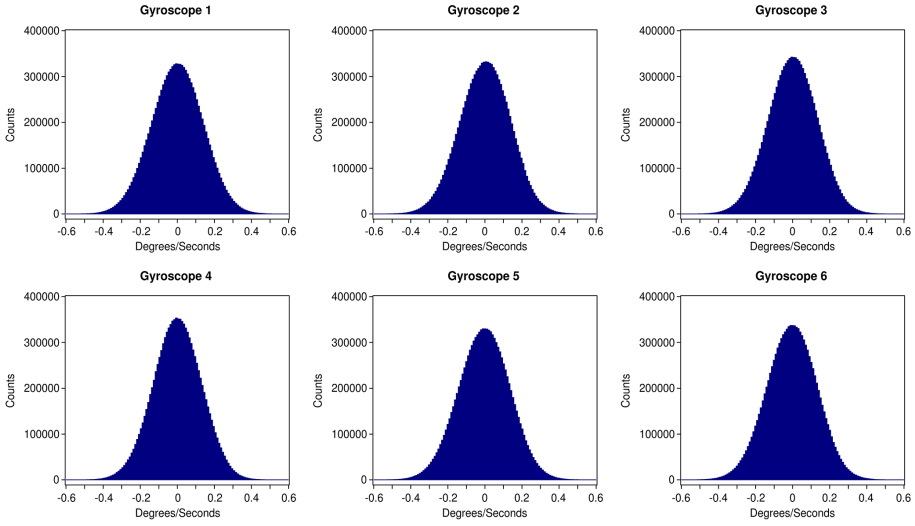

Figure 4. Angular rate histograms of the signals of Fig. 3.

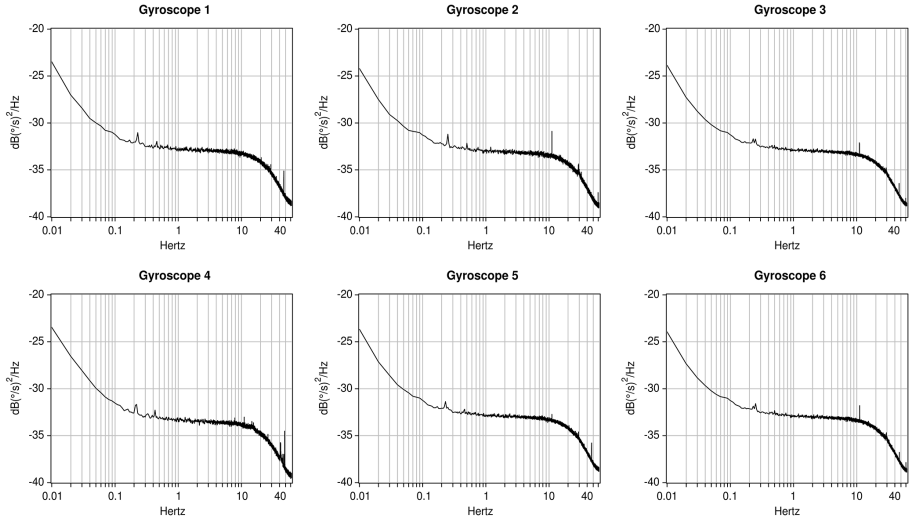

Figure 5. Angular rate PSD of the signals of Fig. 3.

tops, games controllers and mobile phones. Thanks to the great commercial success, the research and development of MEMS technology actively continues all over the world. A MEMS device is a system capable of receiving information from the environment by translating the physical quantities into electrical impulses. The MEMS sensors can measure phenomena of various kinds: mechanical (sound, acceleration and pressure), thermal (temperature and heat flux), biological (cell potential), chemical (pH), optical (intensity of light radiation, spectroscopy), magnetic (intensity of flow). Due to their versatility, MEMS sensors are increasingly being used in a wide field of science, including the physical, engineering, medical and earthquakes (D'Alessandro and D'Anna, 2013; D'Alessandro et al., 2014b; D'Alessandro, 2014b) one.

A gyroscope is a rotating physical device that, due to the law of angular momentum conservation, tends to maintain its rotation axis oriented in a fixed direction. A homogeneous mass, which quickly turns around its principal axis of inertia, develops centrifugal forces that appear to be perfectly in balance among them. In this way, no internal force can disturb the rotational motion and generate vibrations or alterations of the same rotational motion. A gyroscope is therefore an instrument that can be used to measure the angular velocity of a body around a generic axis, respect to an inertial reference system.

The angular velocity can be derived through different physical principles. The MEMS gyroscopes generally exploit the inertial accelerations that arise due to the motion of the sensor with respect to a non-inertial reference system, which

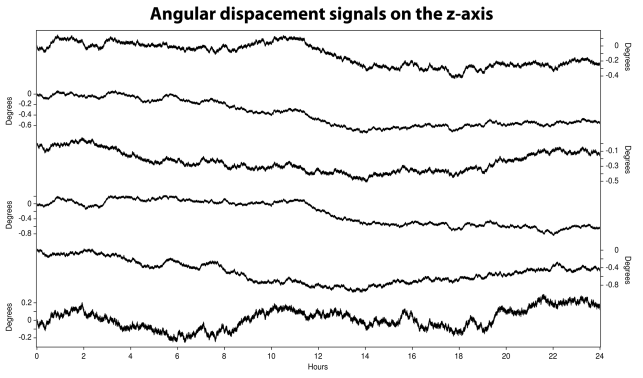

Figure 6. Angular displacement determined from the signals of Fig. 3.

is the Coriolis acceleration. Figure 1 schematised the principle of operation of a MEMS gyroscope. The system consists of two masses joined by means of an elastic element. Subjecting the system to the action of a forcing in the x direction and to the rotation imposed by an angular velocity along the z axis (perpendicular to the xy plane), it manifests the appearance of an acceleration directed orthogonally to the trajectory (in y direction), that is precisely the Coriolis acceleration.

The MEMS device here tested is the model 1044_0 (3/3/3 Phidget Spatial Precision High Resolution) produced by the Canadian company Phidget Inc (Fig. 2). This device integrates a three-axis gyroscope but is also equipped with an accelerometer and a magnetometer, both tri-axial. The sensor was chosen from among hundreds of MEMS gyroscope on the market based on his performance, cost and in relation to the purpose of this paper. The circuit of transduction is internal to the device and is of the digital type, for which the outputs are already in a digital format and proportional to the measured quantity.

The integrated gyroscope features three sensing elements oriented along three mutually orthogonal axes. In precision mode, the gyroscope have resolution of 0.02 and $0.013^\circ\,s^{-1}$ on horizontals and vertical axis, respectively. The self-noise standard deviation is $0.095^\circ\,s^{-1}$ and the maximum measurable angular rate is 300 and $400^\circ\,s^{-1}$ for the horizontals and vertical axis, respectively.

Moreover, the MEMS device has a low current consumption, estimated at a maximum current consumption of 55 mA. Power can be supplied via a USB connection with a potential difference between 4.4 and 5.3 V. The sampling step can be set between a minimum of 4 ms sample^{-1} to a maximum of 1 s sample^{-1}. The analogical to digital conversion is done automatically by means of a 16-bit digital converter. Furthermore, the temperature range of operation is extremely large (-40–$85\,^\circ$C) ensuring the operation of the device even in the most extreme temperature conditions. All specifications above described, together with the small size of the device ($3 \times 3.5 \times 0.4$ cm) and its low cost, make this MEMS device suitable for co-installation with seismic sensor in borehole or in OBS.

3 Performance evaluation

In order to evaluate the performance of the gyroscope included in the MEMS model 1044_0, we have tested six different devices. Since the main aim of this work is to check the suitability of this equipment to retrieve the horizontal components rotation, in that follows, we consider only the signals relative to the vertical (z) axis of the gyroscope. In each of the tests described below the sampling frequency has been set equal to 125 Hz.

The first test was performed in order to verify the parameters declared by the manufacturer on the gyroscope self-noise. The six sensors have been co-installed in a quiet place and signals acquired for a week. Figure 3 show 24 h of signals recoded on the z axis by the six MEMS gyroscopes tested. The recorded signals show the typical features of the self-noise generated by electronic systems. Such self-noise shows good temporal stationarity throughout the whole observation period for all the six sensors tested. Their amplitude histograms show a typical Gaussian distribution (Fig. 4); all the signals have zero mean ($< 10^{-9}\,^\circ\,s^{-1}$) and standard deviation between 0.130 e $0.138\,^\circ\,s^{-1}$, slightly greater than that declared by the manufacturer. The Skewness ranges between -0.026 and -0.042 while the Kurtosis ranges between -0.018 and -0.050.

For our purposes, that is the determination of the sensor horizontal rotation we are interested to the angular displacement. Angular displacement can be determined from angular rate by means of time integration. However, time integration without any data pre-processing can lead to a large drift in the resulting signals. This drift is generated by the very low frequency component of the original signals that, after time integration, as suggest by the theorem of convolution, are largely amplified (each spectral coefficient result divided by the angular frequency).

Figure 5 shows the angular rate Power Spectra Density (PSD) of the signals of Fig. 3. The PSD was calculated using the periodogram method. To calculate the average PSD, each signal was split into half-overlapped time windows 100s long and a Hanning window was applied to each time window to reduce spectrum distortion due to the signals truncation.

We can observe as at very low frequency (< 0.1 Hz) the self-noise generated by the MEMS gyroscopes have high power. To reduce the drift, before time integration to derive angular displacement, we applied a high-pass filter with cut-off frequency of 0.2 Hz.

Figure 6 show the same signals of Fig. 3 after time integration using Simpson's rule. We can observe as the resulting angular displacement signals have little offset (between -0.491 and 0.016°) and standard deviation between 0.115 and 0.320°. These values can be considered respectively as

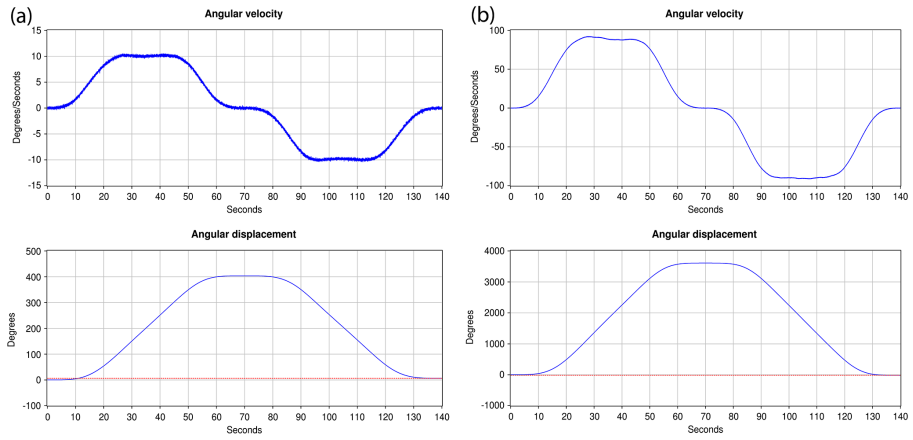

Figure 7. Signals recorded by a MEMS sensor during the rotation test at angular rate of **(a)** 10 and **(b)** 90 ° s^{-1}. The dashed red line indicated the real stop position of the rotating table.

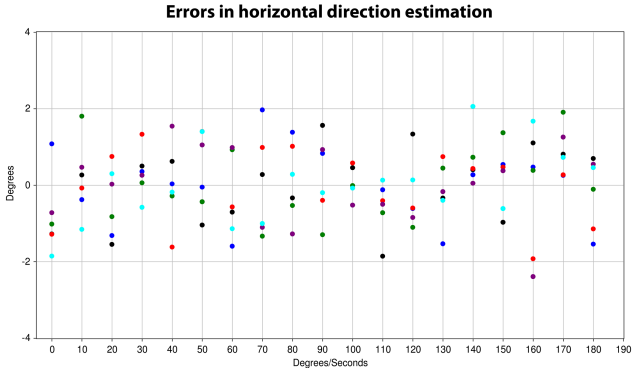

Figure 8. Differences between measured and determined angular displacements as function of the angular rate: black = gyroscope 1, blue = gyroscope 2, red = gyroscope 3, green = gyroscope 4, violet = gyroscope 5, cyan = gyroscope 6.

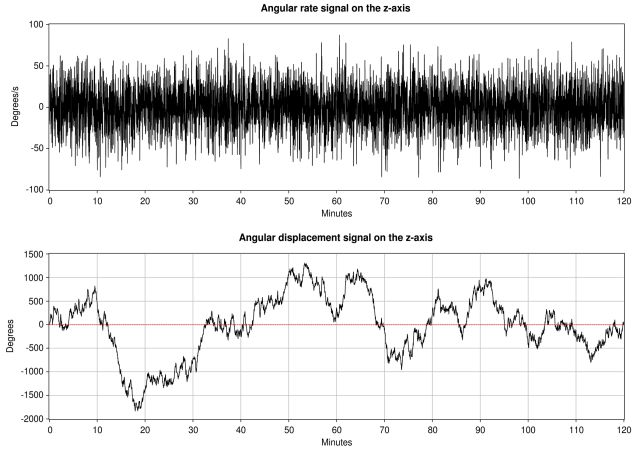

Figure 9. Signals recorded by a MEMS sensor during a random horizontal rotation for a period of 2 h.

a measure of the best accuracy and precision achievable by this instrument when used to derive angular displacements.

The second test was performed in order to verify the ability of the MEMS gyroscope to retrieve angular displacement when it undergoes to a rotation at a given angular velocity. The tests were conducted using a rotating table capable of generating rotation at about constant angular rate. The gyroscopes were subjected, for several tens of seconds, to a rotation on z-axis at constant angular rate, first clockwise and then counter clockwise, to go back to its starting position. The tests were performed generating rotation at angular rate between 0 and 180 ° s^{-1} with step of 10 ° s^{-1}.

Figure 7 show the angular rate and the derived angular displacement signals recorded on the z axis of a MEMS gyroscope subjected to a rotation at angular rate of 10 and 90 ° s^{-1}. Following the angular rate signals of Fig. 7, we can see as from a standing start, the sensor is subjected to a clockwise rotation with increasing angular rate to reach the maximum angular rate (0–20 s), that in the two examples reported in Fig. 7 are 10 and 90 ° s^{-1}. Following the gyroscope is subjected to a clockwise rotation at constant angular rate (20–50 s) and subsequently the angular rate is decreased up to stop the rotation (50–70 s) and the process is symmetrical repeated in counter clockwise (70–140 s).

In this test, the theoretical final angular displacement should be zero, but in reality our rotating table lead the sensor to a position that does not coincide exactly with the initial one (in the figure the final angular displacement is indicated with a red dashed line). For this reason, in each test, the final angular displacement was then measured with a high precision goniometer with angular resolution of 0.1°. For each test, we determined the difference between the final angular displacement measured and that determined from gyroscope signals.

Figure 8 show, for the six tested gyroscope, the differences between the measured and determined angular displacements

as function of the angular rate. We can observe as only in 2 cases out of 114 (2 %) the error is greater than 2°, with mean standard deviation equal to 0.93°.

We can therefore say that, for rotations at angular rate between 0 and 180 $^\circ\,s^{-1}$, the MEMS gyroscope here tested, can used to determine the final angular displacement with error less than 2° in the 98 % of cases.

However, the OBS falling time is generally greater than 140s. From our experience, the OBS falling velocity is between 35–55 m min^{-1} and so for deployment in deep water the fall can last more than an hour. For this reason, in order to simulate the descent phase in the sea of an OBS, we have carried out an additional test. In this last test, we applied to each MEMS sensor a random horizontal rotation for a period of 2 h (Fig. 9). The obtained result is in agreement (error less than 2°) with those of the tests previously carried out. The error does not increase, as it is not linked to the accuracy of the measurements, but only to the presence of the instrument self-noise, which can be considered random and stationary.

4 Conclusions

As well known, the magnitude detection threshold and location performance of a seismic network are mainly related to the noise level and geometry of the stations that make up the network (D'Alessandro et al., 2011a, b, 2012b, 2013b, c, d; D'Alessandro and Stickney, 2012; D'Alessandro and Ruppert, 2012; D'Alessandro and D'Anna, 2013). OBS are increasingly used to monitoring offshore areas while downhole sensors always have been used to reduce natural noise level. However, due to sensor rotation during installation, the absolute orientation of the horizontal components are generally unknown. This can be a major problem that can limit data analysis and interpretation. Indeed, the absolute orientation of the horizontal components is critical for many seismic analysis techniques such as receiver functions, body- and surface-wave polarization, anisotropy and surface wave dispersion analysis.

In this paper, we have proposed a simple method to retrieve ocean bottom and downhole seismic sensors horizontal components orientation using a low cost MEMS gyroscope. We have tested the gyroscope included in the MEMS model 1044_0-3/3/3 produced by the Canadian company Phidget Inc, by means of a rotation table. Our test have showed that this MEMS gyroscope can be used to retrieve angular displacement, by means of simple time integration of the angular rate signals. However, to improve the accuracy is necessary to apply an appropriate high-pass filter to remove the low frequency components generated by the device self-noise. A correct processing of the signals permit to retrieve, for rotation at angular rate between 0 and 180 $^\circ\,s^{-1}$, the final angular displacement with error less 2° in the 98 % of cases, also for long duration rotations (2 h).

It is clear that co-installing the gyroscope with a seismic sensor, this can be used to retrieve the absolute sensor horizontal axis orientation. This technology/method is promising, but clearly will require additional work to make operational.

The next step will be the creation of a stand-alone module equipped with single board computer and a battery pack able to record the signals generated by the gyroscope for several days. The module would be down with the sensor and recovered after the installation for downhole and at the end of the monitor campaign for OBS.

Acknowledgements. We are grateful to the anonymous reviewer, Adam Ringler and the Editor Damiano Pesaresi for their constructive comments and suggestions. Special thanks to Chester Fitchett and the Phidgets Inc. (Canada) which provided free of charge the tested devices.

Edited by: D. Pesaresi
Reviewed by: A. Ringler and one anonymous referee

References

Anderson, P. N., Duennebier, F. K., and Cessaro, R. K.: Ocean borehole horizontal seismic sensor orientation determined from explosive charges, J. Geophys. Res.-Solid Earth, 92, 3573–3579, doi:10.1029/JB092iB05p03573, 1987.

Baker, G. E. and Stevens, J. L.: Backazimuth estimation reliability using surface wave polarization, Geophys. Res. Lett., 31, 1–4, doi:10.1029/2004GL019510, 2004.

Chiu, H. C., Huang, H. C., Leu, C. L., and Ni, S. D.: Application of polarization analysis in correcting the orientation error of a downhole seismometer, Earthquake Eng. Struct. Dynam., 23, 1069–1078, 1994.

D'Alessandro, A., D'Anna, G., Luzio, D., and Mangano, G.: The INGV's new OBS/H: analysis of the signals recorded at the Marsili submarine volcano, J. Volcanol. Geotherm. Res., 183, 17–29, doi:10.1016/j.jvolgeores.2009.02.008, 2009.

D'Alessandro, A., Luzio, D., D'Anna, G., and Mangano, G.: Seismic Network Evaluation through Simulation: An Application to the Italian National Seismic Network, B. Seismol. Soc. Am., 101, 1213–1232, doi:10.1785/0120100066, 2011a.

D'Alessandro, A., Papanastassiou, D., and Baskoutas, I.: Hellenic Unified Seismological Network: an evaluation of its performance through SNES method, Geophys. J. Int., 185, 1417–1430, doi:10.1111/j.1365-246X.2011.05018.x, 2011b.

D'Alessandro, A. and Ruppert, N.: Evaluation of Location Performance and Magnitude of Completeness of Alaska Regional Seismic Network by SNES Method, B. Seismol. Soc. Am., 102, 2098–2115, doi:10.1785/0120110199, 2012.

D'Alessandro, A. and Stickney, M.: Montana Seismic Network Performance: an evaluation through the SNES method, B. Seismol. Soc. Am., 102, 73–87, doi:10.1785/0120100234, 2012.

D'Alessandro, A., Mangano, G., and D'Anna, G.: Evidence of persistent seismo-volcanic activity at Marsili seamount, Ann. Geophys., 55, 213–214, doi:10.4401/ag-5515, 2012a.

D'Alessandro, A., Danet, A., and Grecu, B.: Location Performance and Detection Magnitude Threshold of the Romanian National Seismic Network, Pure Appl. Geophys., 169, 2149–2164, doi:10.1007/s00024-012-0475-7, 2012b.

D'Alessandro, A. and D'Anna, G.: Suitability of low cost 3 axes MEMS accelerometer in strong motion seismology: tests on the LIS331DLH (iPhone) accelerometer, B. Seismol. Soc. Am., 103, 2906–2913, doi:10.1785/0120120287, 2013.

D'Alessandro, A., Mangano, G., D'Anna, G., and Luzio, D.: Waveforms clustering and single-station location of microearthquake multiplets recorded in the northern Sicilian offshore region, Geophys. J. Int., 194, 1789–1809, doi:10.1093/gji/ggt192, 2013a.

D'Alessandro, A., Badal, J., D'Anna, G., Papanastassiou, D., Baskoutas, I., and Özel. M. M.: Location Performance and Detection Threshold of the Spanish National Seismic Network, 1859–1880, Pure Appl. Geophys., 170, 1420–9136, doi:10.1007/s00024-012-0625-y, 2013b.

D'Alessandro, A., Gervasi, A., and Guerra, I.: Evolution and strengthening of the Calabrian Regional Seismic Network, Adv. Geosci., 36, 11–16, doi:10.5194/adgeo-36-11-2013, 2013c.

D'Alessandro, A., Scarfì, L., Scaltrito, A., Di Prima, S., and Rapisarda, S.: Planning the improvement of a seismic network for monitoring active volcanic areas: the experience on Mt. Etna, Adv. Geosci., 36, 39–47, doi:10.5194/adgeo-36-39-2013, 2013d.

D'Alessandro, A.: The Marsili Seamount, the biggest European volcano, could be still active!, Current Sci., 106, p. 1339, 2014a.

D'Alessandro, A.: Monitoring of earthquakes using MEMS sensors, Current Sci., 107, 733–734, 2014b.

D'Alessandro, A., Guerra, I., D'Anna, G., Gervasi, A., Harabaglia, P., Luzio, D., and Stellato, G.: Integration of onshore and offshore seismic arrays to study the seismicity of the Calabrian Region: a two steps automatic procedure for the identification of the best stations geometry, Adv. Geosci., 36, 69–75, doi:10.5194/adgeo-36-69-2014, 2014a.

D'Alessandro, A., Luzio, D., and D'Anna, G.: Urban MEMS based seismic network for post-earthquakes rapid disaster assessment, Adv. Geosci., 40, 1–9, doi:10.5194/adgeo-40-1-2014, 2014b.

Duennebier, F., Anderson, P., and Fryer, G.: Azimuth determination of and from horizontal ocean bottom seismic sensors, J. Geophys. Res., 92, 3567–3572, doi:10.1029/JB092iB05p03567, 1987.

Ekström, G. and Busby, R. W.: Measurements of Seismometer Orientation at USArray Transportable Array and Backbone Stations, Seismol. Res. Lett., 79, 554–561, doi:10.1785/gssrl.79.4.554, 2008.

Grigoli, F., Cesca, S., Dahm, T., and Krieger, L.: A complex linear least-squares method to derive relative and absolute orientations of seismic sensors, Geophys. J. Int., 188, 1243–1254, doi:10.1111/j.1365-246X.2011.05316.x, 2012.

Holcomb, G. L.: Experiments in seismometer azimuth determination by comparing the sensor signal outputs with the signal output of an oriented sensor, USGS Open-File Report: 2002-183, pp. 205, 2002.

Mangano, G., D'Alessandro, A., and D'Anna, G.: Long-term underwater monitoring of seismic areas: design of an Ocean Bottom Seismometer with Hydrophone and its performance evaluation, OCEANS 2011 IEEE Conference, 6–9 June, Santander, Spain, in: OCEANS 2011 IEEE Conference Proceeding, pp. 9, doi:10.1109/Oceans-Spain.2011.6003609, 2011.

Michaels, P.: Use of principal component analysis to determine downhole tool orientation and enhance SH-waves, J. Environ. Eng. Geophys., 6, 175–183, 2001.

Nakamura, Y., Donoho, P. L., Roper, P. H., and McPherson, P. M.: Large offset seismic surveying using ocean-bottom seismographs and air gun: instrumentation and field technique, Geophysics, 52, 1601–1611, 1987.

Oye, V. and Ellsworth, W. L.: Orientation of three-component geophones in the San Andreas fault observatory at depth pilot hole, Parkfield, California, B. Seismol. Soc. Am., 95, 751–758, 2005.

Ringler, A. T., Edwards, J. D., Hutt, C. R., and Shelly, F.: Relative azimuth inversion by way of damped maximum correlation estimates, Comput. Geosci., 43, 1–6, 2012.

Ringler, A. T., Hutt, C. R., Persefield, K., and Gee, L. S.: Seismic Station Installation Orientation Errors at ANSS and IRIS/USGS Stations, Seismol. Res. Lett., 84, 926–931, doi:10.1785/0220130072, 2013.

Stachnik, J. C., Sheehan, A. F., Zietlow, D. W., Yang, Z., Collins, J., and Ferris, A.: Determination of New Zealand Ocean Bottom Seismometer Orientation via Rayleigh-Wave Polarization, Seismol. Res. Lett., 83, 704–713, doi:10.1785/0220110128, 2012.

Zha, Y., Webb, S. C., and Menke, W.: Determining the orientations of ocean bottom seismometers using ambient noise correlation, Geophys. Res. Lett., 40, 1–6, doi:10.1002/grl.50698, 2013.

Zheng, X. and McMechan, G. A.: Two methods for determining geophone orientations from VSP data, Geophysics, 71, 87–97, 2006.